Journal of Dynamics, Monitoring and Diagnostics, 2023, 2, 183-189
https://doi.org/10.37965/jdmd.2023.207

ISTP
RESEARCH ARTICLE

An Improved Second-Order Multisynchrosqueezing Transform for the Analysis of Nonstationary Signals

Kewen Wang, Yajun Shang, Yongzheng Lu, and Tianran Lin
Qingdao Key Rail Transportation Laboratory for Noise and Vibration Control and Automated Fault Diagnostic, Qingdao University of Technology, Qingdao 266525, China

(Received 09 March 2023; Revised 30 April 2023; Accepted 04 August 2023; Published online 15 August 2023)

Abstract: Second-order multisynchrosqueezing transform (SMSST), an effective tool for the analysis of nonstationary signals, can significantly improve the time-frequency resolution of a nonstationary signal. Though the noise energy in the signal can also be enhanced in the transform which can largely affect the characteristic frequency component identification for an accurate fault diagnostic. An improved algorithm termed as an improved second-order multisynchrosqueezing transform (ISMSST) is then proposed in this study to alleviate the problem of noise interference in the analysis of nonstationary signals. In the study, the time-frequency (TF) distribution of a nonstationary signal is calculated first using SMSST, and then a δ function is constructed based on a newly proposed time-frequency operator (TFO) which is then substituted back into SMSST to produce a noise-free time frequency result. The effectiveness of the technique is validated by comparing the TF results obtained using the proposed algorithm and those using other TFA techniques in the analysis of a simulated signal and an experimental data. The result shows that the current technique can render the most accurate TFA result within the TFA techniques employed in this study.

Keywords: fault diagnosis; nonstationary signals; synchrosqueezing transform; time-frequency operator

I. INTRODUCTION

As the most important mechanical component in the power transmission train of a rotating machine, the health condition of the planetary gearbox can largely affect the normal operation of the machine. An effective condition monitoring (CM) and fault diagnosis program in placed can largely prevent potential economic losses caused by the degradation of a critical component fault to ensure a safety operation of a machine [1–3]. CM signals acquired from a rotating machine often demonstrates nonlinear/nonstationary characteristics due to changing load and/or speed during the operation [4,5]. As a result, classical frequency domain analysis techniques such as Fourier transform are inadequate for the analysis of such signals. Time-frequency analysis (TFA), which can reveal both time and frequency information synchronously, was then proposed in the analysis of nonlinear/nonstationary signals to produce an accurate fault diagnostic for machines operating under complicate conditions.

Traditional TFA techniques such as short-time Fourier transform (STFT), wavelet transform (WT), and S-transform (ST) are widely used in the analysis of nonstationary signals though these techniques have certain limitations. For example, STFT performs the Fourier transform of a signal segment within a finite time span defined by a sliding time window by assuming that the signal segment is stationary within the time span [6]. However, due to the fixed window length used in the transform and the Heisenberg uncertainty principle, STFT cannot produce satisfying resolutions in both time and frequency domains. On the other hand, WT can overcome the disadvantage of fixed window length through the usage of the scale parameter and the time translation of a mother wavelet [7]. However, it is difficult to find a suitable mother wavelet to match the signal characteristics. Whereas the window length of the Gaussian window function in ST is inversely proportional to the frequency, it overcomes the defect of a fixed window, though it also leads to the reduced frequency resolution at high frequencies of the result [8].

Many post-processing methods have been developed in recent years to improve the analysis result of TFAs. For instance, the reassignment method (RM) redistributes the time-frequency coefficients to the location of the instantaneous frequency (IF) in both time and frequency directions to improve the readability of the time-frequency distribution [9]. Regretfully, the operation is not reversible where the result cannot be used for signal reconstruction. Synchrosqueezing wavelet transform (SWT), an algorithm proposed originally by Daubechies *et al.*, can squeeze the diffused energy of the WT to the IF along the frequency direction to produce a high energy concentration TF result [10]. Thakur *et al.* extended the algorithm by using an alternative STFT framework in the transform, and the technique was formally termed as synchrosqueezing transform (SST) [11]. Nevertheless, both SWT and SST assume that the analyzed signal is a pure harmonic signal which can lead to a large deviation in the estimated IF and a smeared time-frequency result when dealing with strong time-varying signals. In addition, the algorithm is also sensitive to noise, which limits its usefulness in many practical application cases. Higher order SST algorithms were then proposed in dealing with strong time-varying signals by the usage of higher-order operators in the transform [12,13]. However, with the increased order of the kernel function, the computation cost will also increase significantly. For example, a first-order SST only needs to perform the STFT once, while a fourth order SST needs to perform the STFT 11 times in the transform. Inspired by the success of SST, a so-called synchroextracting transform (SET) was proposed

Corresponding author: Tianran Lin (e-mail: trlin@qut.edu.cn).

by Yu *et al.* [14] which allocates the time-frequency coefficients directly to the trajectory of the IF when the frequency matches the estimated IF obtained by the partial derivative of the STFT. Nevertheless, because the IF estimator is calculated based on the assumption of quasi-stationarity signals, the algorithm is not suitable in the handling of strong time-varying signals. Whereas Yu *et al.* [15] combined a chirplet function with the SET and an iterative process to produce a higher energy concentrated TF result in the analysis of signals with rapid changing dynamics. Yu *et al.* [16] proposed a multi-synchrosqueezing transform (MSST) by using an iterative process to squeeze the diverged energy repeatedly into the IF trajectories. Furthermore, Yu *et al.* [17] introduced a second-order IF estimator into the MSST (termed as SMSST) to capture the rapid changing IF in the analysis of a rotor defect signal. Yet it is also noted that the noise in the signal is also squeezed during the iterative process leading to a poor readability of the TF result when the analyzed signal is contaminated by strong noise. In order to alleviate the noise interference, Li *et al.* [18] combined a ridge extraction (RE) and a MSST where the defect frequency components from the MSST are extracted by the RE algorithm and then reconstructed to produce a noise-free TF result. The effectiveness of the algorithm was verified in the study in the analysis of an experimental bearing defect data. However, the IFs of the defect frequency components in the signal need to be extracted individually which would be very time consuming when dealing with signals containing multiple frequency components. To further improve the TF resolution and the noise robustness of the SMSST in the analysis of noise contaminated time-varying signals, an improved second-order multi-synchrosqueezing transform (ISMSST) is proposed in this study. Under this approach, a new δ function is constructed based on a newly proposed time-frequency operator (TFO) which is then substituted back into a SMSST algorithm to produce a time frequency result free of noise interference in the analysis of a strong nonstationary signal with rapidly changing speed. The effectiveness of the proposed algorithm is validated in a comparison study with other TF algorithms which shows that the present technique can produce a better, high quality TF result for an accurate mechanical fault diagnosis.

The rest of the paper is arranged as follows: In Section II, the theoretical basis of SST, SMSST, and the ISMSST technique proposed in this study is briefly reviewed. In Section III and Section IV, two case studies (a simulated multicomponent nonstationary signal and an experimental gearbox defect data under varying speed condition) are presented where the effectiveness of the current technique is verified by comparing the TF results obtained from the current technique with those obtained using other commonly employed TFA techniques. Finally, conclusions are drawn in Section V.

II. THE BASIC THEORY

A. A SYNCHROSQUEEZING TRANSFORM (SST)

For a time-varying signal $x(t)$, its STFT can be expressed as

$$STFT(t,\omega) = \int_{-\infty}^{+\infty} x(u) \cdot g(u-t) \cdot \mathrm{e}^{-\mathrm{j}\omega u} du, \quad (1)$$

where $g(u\text{-}t)$ is the sliding time window function.

By incorporating an additional phase shift $e^{j\omega t}$ in the transform [14], Equation (1) can be rewritten as

$$STFT_e(t,\omega) = \int_{-\infty}^{+\infty} x(u) \cdot g(u-t) \cdot \mathrm{e}^{-\mathrm{j}\omega(u-t)} du. \quad (2)$$

Equation (2) can also be written as

$$STFT_e(t,\omega) = \frac{1}{2\pi} \int_{-\infty}^{+\infty} \widehat{x}(\xi) \cdot \widehat{g}(\omega-\xi) \cdot \mathrm{e}^{\mathrm{j}\xi t} d\xi, \quad (3)$$

where $\widehat{x}(\xi)$ is the Fourier transform of $x(u)$, and $\widehat{g}(\omega-\xi)$ is the Fourier transform of $g(u-t)$.

Now, considering that the signal is a single-component pure harmonic signal given by

$$x(t) = A \cdot \mathrm{e}^{\mathrm{j}\omega_0 t}, \quad (4)$$

its STFT is

$$STFT_e(t,\omega) = A \cdot \widehat{g}(\omega-\omega_0) \cdot \mathrm{e}^{\mathrm{j}\omega_0 t}. \quad (5)$$

The IF of the signal can now be calculated by taking a partial derivative (∂_t) of Equation (5) in respect with time as

$$\begin{aligned} \partial_t STFT_e(t,\omega) &= \partial_t (A \cdot \widehat{g}(\omega-\omega_0) \cdot \mathrm{e}^{\mathrm{j}\omega_0 t}) \\ &= STFT_e(t,\omega) \cdot j \cdot \omega_0. \end{aligned} \quad (6)$$

From Equation (6), for any TF point (t,ω) and for $STFT_e(t,\omega) \neq 0$, the two-dimensional IF of the signal in the TF plane can be estimated as

$$\omega_0(t,\omega) = -j \cdot \frac{\partial_t STFT_e(t,\omega)}{STFT_e(t,\omega)}. \quad (7)$$

SST of the signal can now be formulated as

$$SST(t,\omega) = \int_{-\infty}^{+\infty} STFT_e(t,\omega) \cdot \delta(\omega-\omega_0) d\omega. \quad (8)$$

B. A SECOND-ORDER MULTISYNCHROSQUEEZING TRANSFORM (SMSST)

The signal model used in SST is a pure harmonic signal, which is based on a quasi-stationary assumption. However, signals from practical sources often demonstrate strong time-varying characteristics where the IF estimator described by Equation (7) would yield a large deviation from the real IF which can then lead to a diverged energy in the TF plane. While a second-order IF estimator uses a second-order function to match the phase change of a strong time-varying signal, which can be expressed as

$$\omega_0^2(t,\omega) = \omega_0(t,\omega) + q\widehat{(t,\omega)}(t - \widehat{t}(t,\omega)), \quad (9)$$

where $q\widehat{(t,\omega)}$ is the local complex modulation operator, and $\widehat{t}(t,\omega)$ is the time-reassignment operator. Substituting Equation (9) into Equation (8), the second-order SST algorithm can be expressed as

$$SSST(t,\omega) = \int_{-\infty}^{+\infty} STFT_e(t,\omega) \cdot \delta(\omega - \omega_0^2(t,\omega)) d\omega. \quad (10)$$

Considering that the TF energy of SSST can be further squeezed into the TF trajectories by the transform, an iterative process can be further applied such that:

$$SSST^{[2]}(t,\omega) = \int_{-\infty}^{+\infty} SSST(t,\omega) \cdot \delta(\omega - \omega_1^2(t,\omega))d\omega$$
$$SSST^{[3]}(t,\omega) = \int_{-\infty}^{+\infty} SSST^{[2]}(t,\omega) \cdot \delta(\omega - \omega_2^2(t,\omega))d\omega$$
$$\vdots$$
$$SMSST(t,\omega) = \int_{-\infty}^{+\infty} SSST^{[N-1]}(t,\omega) \cdot \delta(\omega - \omega_N^2(t,\omega))d\omega \tag{11}$$

where $SMSST(t,\omega)$ is the result of $SSST(t,\omega)$ after N^{th} iterations.

C. AN IMPROVE SECOND-ORDER MULTISYNCHROSQUEEZING TRANSFORM (ISMSST)

It can be seen from Equations (9) to (11) that the SMSST can render a high accurate result in analyzing a strong time-varying signal by using a second-order IF estimator and an iterative process. However, the noise in the signal will also be squeezed, which can seriously affect the readability of the time-frequency result.

To address this issue, a new TFO is defined in this study as

$$TFO(t,\omega) = \begin{cases} 1, & if\ SMSST(t,\omega) > \beta \\ 0, & \text{otherwise} \end{cases}, \tag{12}$$

where β is the energy threshold, and its value is set to the averaged energy in the frequency direction at each time instant according to reference [19]. Considering that the signal from a practical application is most likely a multi-component signal, the energy threshold can be modified by a weight factor which value is the number of components k in this study.

Based on the above analysis, the TF points on the entire TF plane can be reproduced by using the new TFO operator which is then substituted back into the SMSST to alleviate the noise interference as

$$ISMSST(t,\omega) = \int_{-\infty}^{+\infty} SMSST(t,\omega) \cdot \delta(\omega - TFO(t,\omega))d\omega. \tag{13}$$

Equation (13) ensures that the TF representation from the transform of a strong time-varying signal will approach that of the ideal TFA of the signal. The algorithm also retains the signal reconstruct ability as illustrated by

$$x(t,\omega) = (2\pi g(0))^{-1} \int_{-\infty}^{+\infty} ISMSST(t,\omega)d\omega. \tag{14}$$

III. NUMERICAL ANALYSIS

Assuming a multi-component nonstationary signal given by

$$x(t) = 2\sin\left[2\pi(17t + 6\sin(1.5t))\right] + 2\sin\left[2\pi(27t + 6\sin(1.5t))\right] + \zeta, \tag{15}$$

its time domain waveform before and after adding noise is shown in Fig. 1(a) and (b). In Equation (15), ζ is the added white Gaussian noise which is set at -2 dB. The sampling frequency of the time waveform is set to 100 Hz, and the sampling time is 4 s.

Fourier transform is applied to the noise added signal described by Fig. 1(b), and the frequency spectrum of the noise added signal is shown in Fig. 2. Not much information can be gained from the frequency spectrum of the signal due to the strong time-varying characteristic of the simulated signal and the interference of the added noise.

Figure 3 compares the time-frequency results of the noise added signal using STFT, SST, SSST, SET, LMSST, MSST, SMSST and the proposed technique. It is shown in Fig. 3(a) that the TF energies of the two signal components are diffused around the IFs of the components by using STFT. While Fig. 3(b) shows that the TF energies from the SST are largely squeezed into the estimated IF trajectories of the two components, though the TF result still suffers from a poor resolution due to the inaccuracy in the IF estimation. The result shown in Fig. 3(c) indicates that SSST renders a more accurate IF estimation due to the use of the second-order operator in the transform. However, the TF energy distribution is still not ideal due to the interference of the added noise. On the other hand, Fig. 3(d)–(f) shows that due to the inaccuracy in the IF estimation using a linear operator, discrepancies are presented in the IF trajectories of the two time-varying signal components in the TF result. An improved IF estimation using a second-order estimator in SMSST leads to a smoother IF trajectories in the TF result as shown in Fig. 3(g) though the noise interference can still be observed. Fig. 3(h) shows that the proposed ISMSST algorithm can produce a noise-free and highly energy concentrated TF result in the analysis of the noise added multicomponent time-varying signal due to the technical enhancement mentioned above.

Figure 4 shows a slice of the TF results at the time instant of 1 second using SST, SSST, SET, LMSST, SMSST, and ISMSST. It is shown in Fig. 4(f) that the frequency spectrum at the time instant from the ISMSST is free from the noise interference, and the signal energies of two components are well preserved from the transform. In contrast, the results from other techniques are either

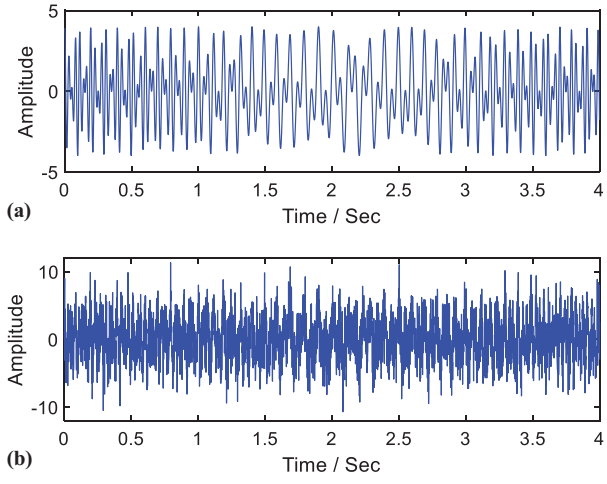

Fig. 1. The time domain of the simulation signal (a) the simulated signal and (b) the noise added signal.

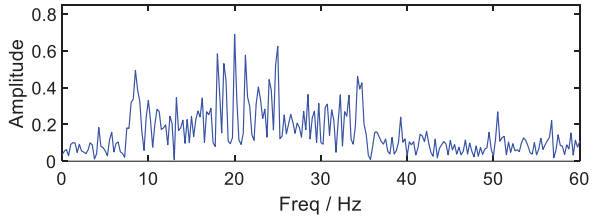

Fig. 2. The frequency spectrum of the noise added signal.

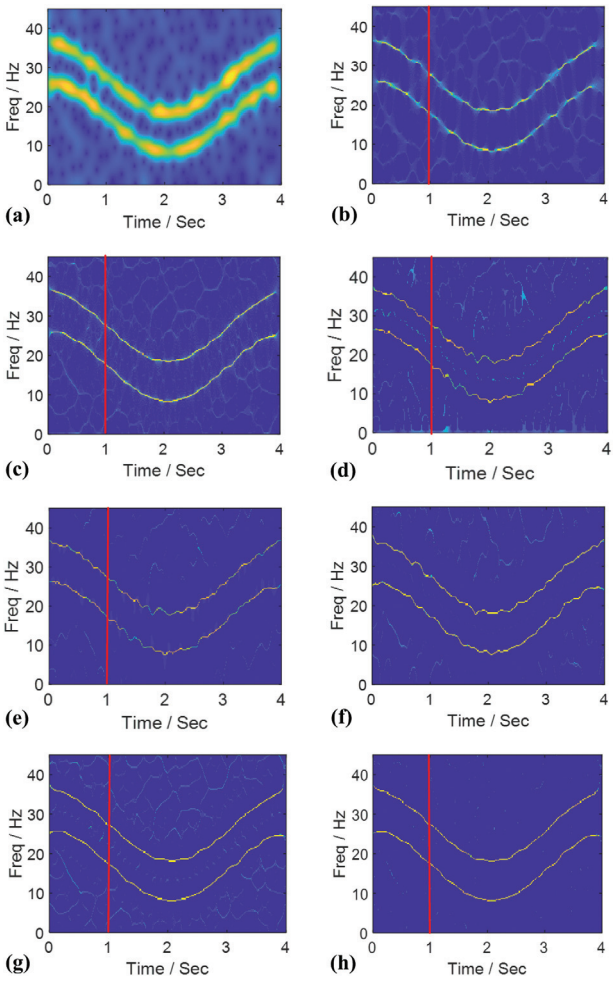

Fig. 3. The TFA results of (a) STFT, (b) SST, (c) SSST, (d) SET, (e) LMSST, (f) MSST, (g) SMSST, and (h) ISMSST.

suffered from a noise interference or an attenuation of the signal amplitude.

A robustness test is also carried out in the study by comparing the Rényi entropies calculated from the TF results of the noise added signal with different signal-to-noise ratio (SNR) using the eight TFA techniques, which are shown in Fig. 5. A lower Rényi entropy indicates that the TFA algorithm can yield a more energy-concentrated TF result [20]. It is shown that the Rényi entropies of the TF results from all algorithms increase as the noise interference increase (i.e., a small SNR). Nevertheless, the Rényi entropy of the TF result calculated using the proposed algorithm is always the lowest regardless of the noise interference level.

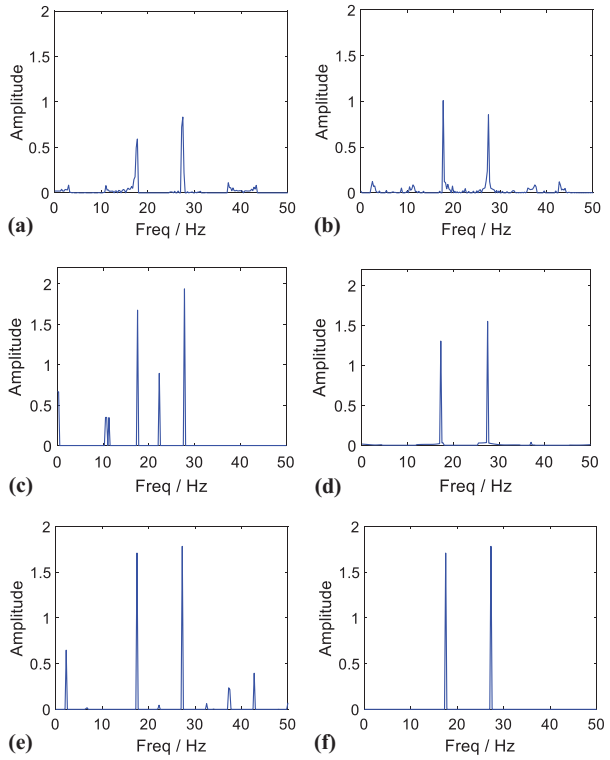

Fig. 4. The TF slices at the time instant of 1 second (a) SST, (b) SSST, (c) SET, (d) LMSST, (e) SMSST, and (f) ISMSST.

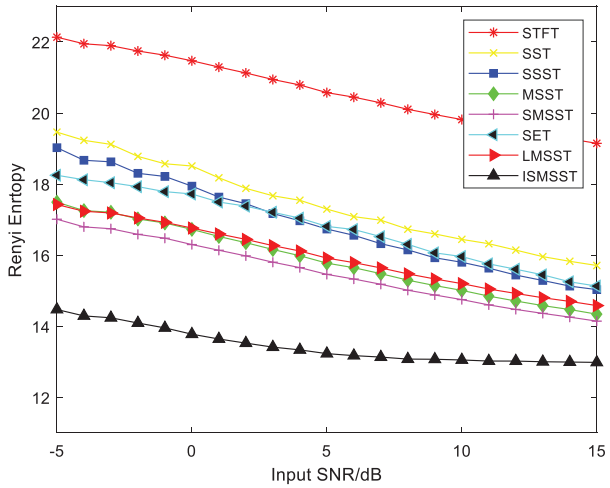

Fig. 5. The Rényi entropies of the TF results under different SNRs calculated using various TFA techniques.

IV. EXPERIMENTAL DATA ANALYSIS

In this section, a gearbox defect data acquired under varying speed condition are used to examine the effectiveness of the proposed technique. Figure 6 shows the experimental test rig (HOUDE METERS HD-CL-05) of the defect planetary gearbox and the data acquisition setting. The test rig consists of a main drive motor with a variable speed controller, a planetary gearbox, a fixed shaft gearbox, and a load motor. A simulated missing tooth fault sun gear is used in the experiment, which is shown in Fig. 7. The gear defect signal is acquired using the accelerometer mounted on the top of

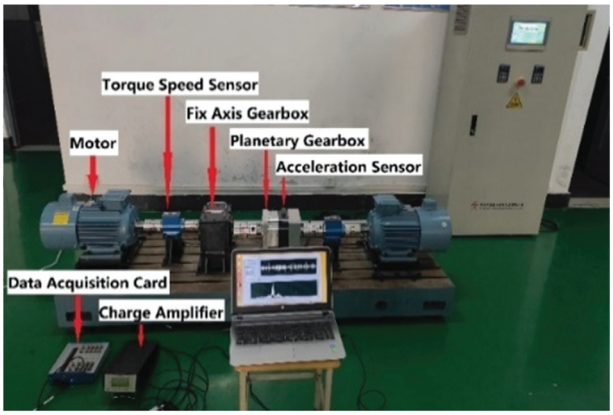

Fig. 6. The experimental test rig of the planetary gearbox.

Fig. 7. A simulated missing tooth fault of the sun gear.

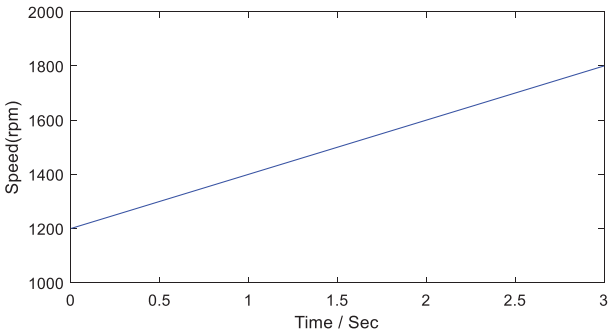

Fig. 8. The shaft speed profile during the experiment.

the planetary gearbox. During the data acquisition, the shaft speed was increased from 1200 RPM to 1800 RPM within 3 seconds, which profile is shown in Fig. 8. The sampling

Table I. The characteristic defect frequency of the sun gear

Motor speed (f_r)	Sun gear rotating frequency (f_s^r)	Sun gear characteristic defect frequency (f_s)
20 – 30 Hz	f_r	$3f_r$

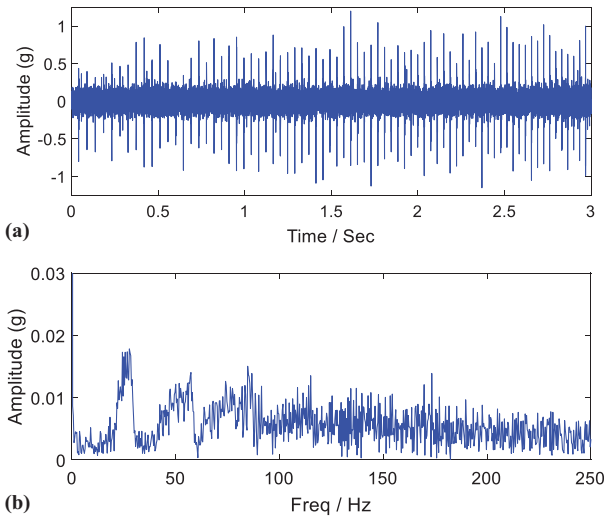

Fig. 9. The gear defect signal (a) the time waveform, (b) the envelope spectrum.

frequency used in the data acquisition is set to 10 kHz. The characteristic defect frequency of the sun gear is shown in Table I.

The time waveform of the measured vibration signal and the envelope spectrum are shown in Fig. 9. It is shown in Fig. 9(b) that the no discrete defect frequency component can be directly extracted from the envelope spectrum due to the speed variation of the test rig in the experiment.

Figure 10(a)–(f) compare the TFA results of the gear defect signal using various TFA techniques. It is shown that

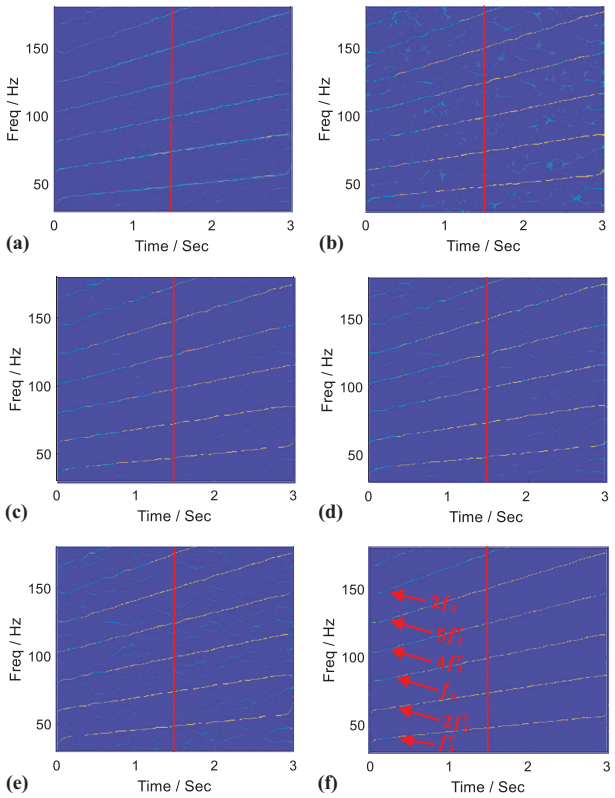

Fig. 10. The TFA results of (a) SSST, (b) SET, (c) LMSST, (d) MSST, (e) SMSST, and (f) ISMSST.

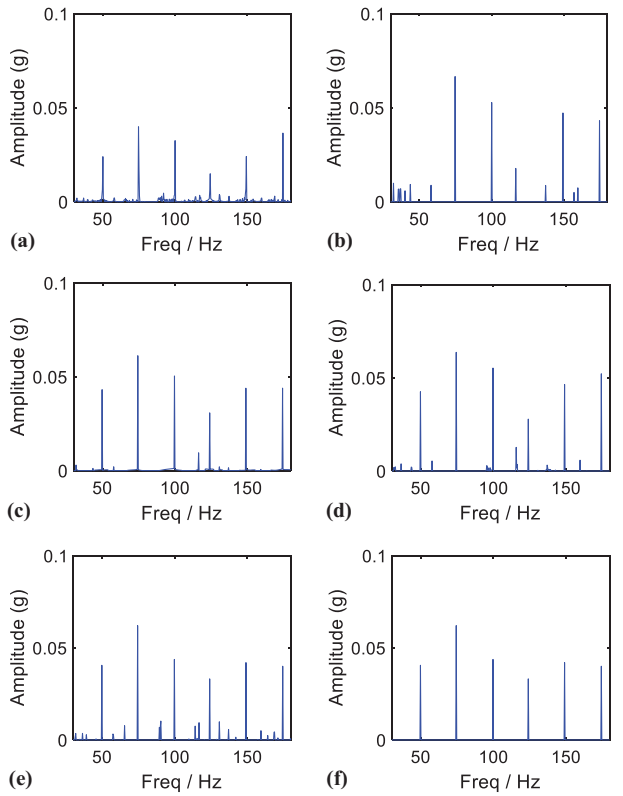

Fig. 11. The TF slices at 1.5 sec (a) SSST, (b) SET, (c) LMSST, (d) MSST, (e) SMSST, and (f) ISMSST.

Table II. The Renyi entropies of the TF results using different TF techniques

SSST	SET	LMSST
15.91	15.22	16.26
MSST	SMSST	ISMSST
16.05	16.62	14.83

the gear defect frequency components and its higher harmonics can be detected from the TFA results using these TFA techniques. However, noise pollution can also be observed of the TF results using the TF techniques other than the proposed technique, which can become serious and affect the accuracy of diagnosis when the SNR of the signal is low. Figure 10(f) shows the proposed technique can produce a noise-free, energy concentrated TF result from noise contaminated nonstationary signals for an accurate machine fault diagnosis.

The slices of the TF representation at the time instant of 1.5 second from Fig. 10 are shown in Fig. 11. It is shown that the frequency spectrum at the time instant from the TF result using the proposed technique is free from the noise interference, and the signal energies of the defect components are well preserved from the transform. On the contrary, the frequency spectra from the slice of the TF results of the other algorithms are affected by the side bands caused by noise interference and an amplitude attenuation of the defect signal components. Furthermore, the comparison of the Rényi entropies calculated from the TF results using the six TF techniques as shown in Table II indicates that the proposed technique can produce a better energy-concentrated TF result than the other TF techniques.

V. CONCLUSION

In this study, an ISMSST technique was proposed for the analysis of noise contaminated time-varying signals. The IFs of a strong time-varying signal were estimated first using a second-order IF estimator, and the signal energies were squeezed into the estimated IF trajectories using an iterative process to produce an energy concentrated TF representation. Finally, a new TFO was proposed to be used in the SMSST to alleviate the noise interference in the TF result.

The validity of the proposed technique was verified in the analysis of a simulated multicomponent time-varying signal and an experimental gear defect signal. It was shown that the proposed algorithm can accurately capture the changing IFs to produce an energy concentrated TF result as well as remove the noise interference in the signal.

The effectiveness of the proposed technique was examined in a comparison study by comparing the TF results with those obtained using other commonly employed TFA techniques. It was shown that the proposed algorithm can produce a better energy concentrated and noise-free TF result than the others in the analysis of noise contaminated time-varying signals.

CONFLICT OF INTEREST STATEMENT

The authors declare no conflicts of interest.

REFERENCES

[1] T. R. Lin *et al.*, "A practical signal processing approach for condition monitoring of low speed machinery using Peak-Hold-Down-Sample algorithm," *Mech. Syst. Signal Process.*, vol. 36, no. 2, pp. 256–270, 2013.

[2] Z. P. Feng *et al.*, "Iterative generalized synchros-queezing transform for fault diagnosis of wind turbine planetary gearbox under nonstationary conditions," *Mech. Syst. Signal Process.*, vol. 52–53, pp. 360–375, 2015.

[3] H. T. Shi *et al.*, "Research on early fault diagnosis method of rolling bearing based on second-order cyclic autocorrelation and DCAE combined with transfer learning," *IEEE Trans. Instrum. Meas.*, vol. 71, pp. 1–18, 2021.

[4] G. Yu *et al.*, "Local maximum synchrosqueezing transform: an energy-concentrated time-frequency analysis tool," *Mech. Syst. Signal Process.*, vol. 117, pp. 537–552, 2019.

[5] Y. Chang *et al.*, "Improved VMD-KFCM algorithm for the fault diagnosis of rolling bearing vibration signals," *IET Signal Process.*, vol. 15, no. 4, pp. 238–250, 2021.

[6] P. Flandrin, "Wavelet analysis and synthesis of fractional Brownian motion," *IEEE Trans. Inf. Theory*, vol. 38, no. 2, pp. 910–917, 1992.

[7] A. Kumar *et al.*, "Research on early fault diagnosis method of rolling bearing based on second-order cyclic autocorrelation and DCAE combined with transfer learning," *IEEE Trans. Instrum. Meas.*, vol. 71, pp. 1–18, 2021.

[8] R. G. Stockwell et al., "Localization of the complex spectrum: the S transform," *IEEE Trans. Signal Process.*, vol. 44, no. 4, pp. 998–1001, 1996.

[9] S. Meignen *et al*., "Time-frequency reassignment and synchrosqueezing," *IEEE Trans. Signal Process.*, vol. 30, pp. 32–41, 2013.

[10] I. Daubechies *et al.*, "Synchrosqueezed wavelet transforms: an empirical mode decomposition-like tool," *Appl. Comput. Harmon. Anal.*, vol. 30, no. 2, pp. 243–261, 2011.

[11] G. Thakur *et al.*, "Synchrosqueezing-based recovery of instantaneous frequency from nonuniform samples," *SIAM J. Math. Anal.*, vol. 43, no. 5, pp. 2078–2095, 2011.

[12] R. Behera *et al.*, "Theoretical analysis of the second-order synchrosqueezing transform," *Appl. Comput. Harmon. Anal.*, vol. 45, no. 2, pp. 379–404, 2018.

[13] D. H. Pham *et al.*, "High-order synchrosqueezing transform for multicomponent signals analysis-with an application to gravitational-wave signal," *IEEE Trans. Signal Process.*, vol. 63, pp. 1335–1344, 2015.

[14] G. Yu *et al.*, "Synchroextracting transform," *IEEE Trans. Signal Process.*, vol. 65, no. 12, pp. 3168–3178, 2017.

[15] K. Yu *et al.*, "A combined polynomial Chirplet transform and synchroextracting technique for analyzing nonstationary signals of rotating machinery," *IEEE Trans. Instrum. Meas.*, vol. 1, no. 1, p. 99, 2019.

[16] G. Yu *et al.*, "Multisynchrosqueezing transform," *IEEE Trans. Instrum. Meas.*, vol. 66, no. 10, pp. 5441–5455, 2019.

[17] K. Yu *et al.*, "Second order multi-synchrosqueezing transform for rub-impact detection of rotor systems," *Mech. Mach. Theory*, vol. 140, pp. 341–349, 2019.

[18] J. X. Li *et al.*, "A multi-synchrosqueezing ridge extraction transform for the analysis of non-stationary multi-component signals," *2021 Global Reliab. Progn. Health Manag.*, vol. 1, pp. 1–5, 2021.

[19] G. Yu *et al.*, "Time-reassigned multisynchrosqueezing transform for bearing fault diagnosis of rotating machinery," *IEEE Trans. Instrum. Meas.*, vol. 1, p. 99, 2020.

[20] G. Yu *et al.*, "Second order transient extracting transform for the analysis of impulse-like signals," *Mech. Syst. Signal Process.*, vol. 147, p. 107069, 2021.